Journal of Alloys and Compounds 509 (2011) 4191–4197

Contents lists available at ScienceDirect

Journal of Alloys and Compounds

journal homepage: www.elsevier.com/locate/jallcom

Theoretical prediction of Grüneisen parameter for bulk metallic glasses

Anjani K. Pandey[a,*], B.K. Pandey[b], Rahul[c]

[a] Deptt. of Physics, Virendra Swarup Memorial Trust Group of Institutions, Unnao, India
[b] Deptt. of Applied Science, Madan Mohan Malaviya Engineering College, Gurakhpur, India
[c] Deptt. of Physics, Dr. M.C. Saxena College of Engineering and Technology, Lucknow, India

ARTICLE INFO

Article history:
Received 28 July 2010
Accepted 17 November 2010
Available online 26 November 2010

PACS:
64.10.+h
65.80.+n
62.20.−x
31.15.−p

Keywords:
EOS
BMG's
Isothermal bulk modulus
Grüneisen parameter

ABSTRACT

The Grüneisen parameter (γ) is of considerable importance to Earth scientists because it sets limitations on the thermo elastic properties of the lower mantle and core. However, there are several formulations of the Grüneisen parameter in frequent use which not only give different values for Grüneisen parameter at ambient pressure but also predict a varying dependence of Grüneisen parameter as a function of compression. The Grüneisen parameter is directly related to the equation of state (EOS), yet it is often the case that both the form of and the EOS are chosen independently of each other and somewhat arbitrarily. In this paper we have assessed some of the more common definitions of the Grüneisen parameter and the EOS's, and have applied them to test the validity of EOS for six different bulk metallic glasses.

1. Introduction

Metallic amorphous alloys (i.e. metallic glasses) are comparatively newcomers to the amorphous materials group. The formation of the first metallic glass of $Au_{75}Si_{25}$ was reported by Duwez's and coworkers [1]. They developed the rapid quenching techniques for chilling metallic liquids at very high rates of 105–106 K/s. Their work showed that the process of nucleation and growth of crystalline phase could be kinetically bypassed in some alloy melts to yield a frozen liquid configuration, i.e. metallic glass. The significance of Duwez's work was that their method permits large quantities of an alloy to be made into glassy state comparing to other methods, for instance, vapour condensation. Formation, structure and property investigations of metallic glasses have attracted increasing attention because of their fundamental scientific importance and engineering application potential [2–5]. The techniques of melt quenching have been extensively developed and elaborated for the purpose of producing a wide variety of metallic glasses.

The research on metallic glasses gained more momentum in the early 1970s and 1980s when the continuous casting processes for commercial manufacture of metallic glasses, ribbons, lines and sheets [5] were developed. An explosion of academic and industrial research has resulted in that period. However, the high cooling rate limited the amorphous alloys geometry to thin sheets and lines, which are unlikely to find wide applications.

When a metal melt is cooled, one of the two events may occur, either crystallization may takes place at melting point or else melt will become more viscous below the melting point with decreasing temperature and may ultimately form amorphous solid, i.e. metallic glasses. Thus, the solid or metallic glass state can be considered as the result of structural freezing of a liquid metal. The discovery of a complex multi-component bulk metallic glass (BMG) has stimulated great interest in various phenomena which was difficult to explain earlier. The large size and high thermal stability of BMGs allow a detailed and accurate study of their various properties over a large temperature and pressure ranges.

Metallic glasses differ in structure and properties from metals. Metals normally have a crystalline structure with atoms in periodic arrays called lattice. In contrast, atoms in glassy metals do not form periodic arrays; their distribution is random. Originally devised a quarter of a century ago, the technique to produce amorphous or glassy metals required cooling of the molten metal about one hundred thousand times faster than had previously been possible.

Rapid cooling was the only way to prevent mobile atoms in the molten metal from rearranging themselves into crystal lattice. Recently [4] it has been discovered, that metallic glasses can be synthesized at low temperatures without quenching by directly introducing certain rapidly diffusing species into crystalline mate-

* Corresponding author at: Deptt. of Physics, Dr. Virendra Swarup Memorial Trust Group of Institutions,Rajendra Swarup Knowledge city, Kanpur-Lucknow Natioanl highway, NH-25, Unnao, India. Tel.: +91 5224009551.
E-mail address: anjani_phys@yahoo.in (A.K. Pandey).

0925-8388/$ – see front matter © 2010 Elsevier B.V. All rights reserved.
doi:10.1016/j.jallcom.2010.11.120

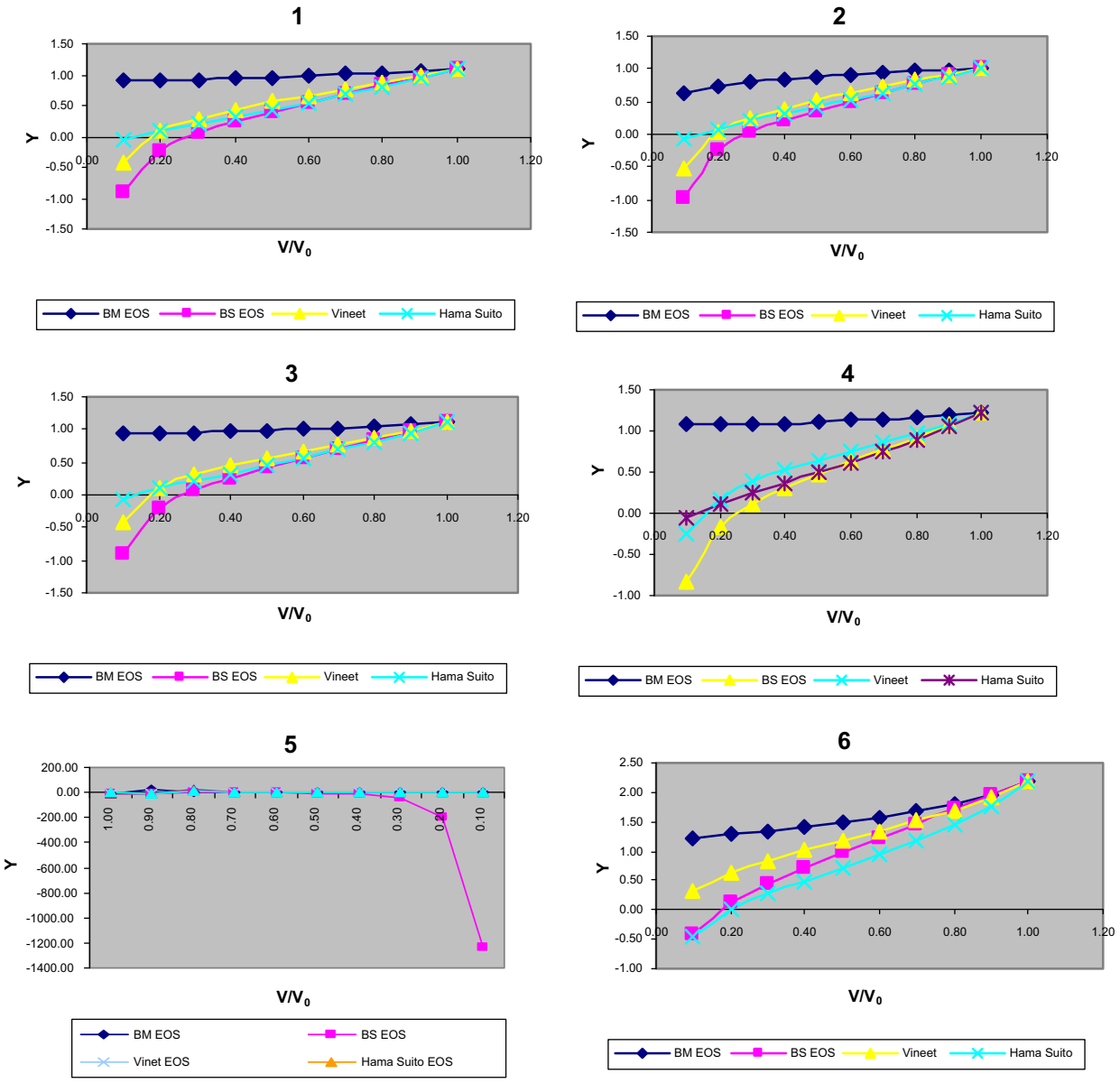

Figs. 1–6. Variation of Grüneisen parameter with compressibility for different bulk metallic glasses. [(**1**) $Zr_{41}Ti_{14}Cu_{12.5}Ni_{10}Be_{22.5}$, (**2**) $Zr_{41}Ti_{14}Cu_{12.5}Ni_{9}Be_{22.5}C_1$, (**3**) $Zr_{40}Nb_3Cu_{12}Fe_8Be_{24}$, (**4**) $(Zr_{0.59}Ti_{0.06}Cu_{0.22}Ni_{0.13})_{0.57}Al_{14.3}$, (**5**) $SiO_2{\cdot}TiO_2$, (**6**) $Pd_{39}Ni_{10}Cu_{30}P_{21}$].

rials. Systems studied so far include hydrogen diffusion in some intermetallic compounds, gold diffusion in lanthanum, nickel diffusion in zirconium metal and others. The common process in all of these systems is that one of the elements, viz., hydrogen, gold and nickel in the above examples, diffuses very rapidly in the other at low temperatures. The rapidly diffusing species induces a phase instability which, because of the low temperatures, results in an amorphous structure rather than a crystalline structure.

However, the understanding of pressure effect in these processes is still remains on a very qualitative level because of the lack of quantitative properties of the compressed metallic glassy state under high pressure. A fundamental understanding of micro structural configuration properties in amorphous solid is not developed in comparison to that of crystalline structure. Due to large size and high thermal stability of BMGs, detailed and accurate study of various properties over a wide temperature and pressure ranges becomes possible. The studies of the acoustic, elastic and thermal properties of metallic glasses can provide important information about the structural and vibrational characteristics [6–8].

With the development of high pressure techniques, pressure is becomes an important processing variable just like that of temperature or chemical composition for condensed phases. High pressure, which can cause a larger change of atom spacing, chemical bonding and Gibbs free energy, has been found to be a powerful tool for affecting and controlling the nucleation and growth in the metallic glasses [9,10]. For example, BMGs can be crystallized under high pressure to very fine-grained nanostructure materials since high pressure can promote local atomic rearrangement and suppress the long-range atomic diffusion in super cooled liquid state. Contamination and grain growth could be avoided in the nano structured material derived from BMG [11] that often occur during consolidation of nanoparticles.

The Grüneisen parameter (γ) has considerable appeal to geophysicists because it is an approximately constant, dimensionless parameter that varies slowly as a function of pressure and temperature. It has both a microscopic and macroscopic definition, the former relating it to the vibrational frequencies of atoms in a material, and the latter relating it to familiar thermodynamic properties

Table 1
Input value of isothermal bulk modulus (K_0) and its pressure derivative (K_0') for bulk metallic glasses [27].

S. no.	BMG's	K_0 (GPa)	K_0' (GPa)
1	$Zr_{41}Ti_{14}Cu_{12.5}Ni_{10}Be_{22.5}$	114.10	4.06
2	$Zr_{41}Ti_{14}Cu_{12.5}Ni_{9}Be_{22.5}C_1$	107.30	3.94
3	$Zr_{40}Nb_3Cu_{12}Fe_8Be_{24}$	113.60	4.10
4	$(Zr_{0.59}Ti_{0.06}Cu_{0.22}Ni_{0.13})_{0.57}Al_{14.3}$	112.60	4.34
5	$SiO_2{\cdot}TiO_2$	34.20	−7.71
6	$Pd_{39}Ni_{10}Cu_{30}P_{21}$	159.10	6.28

such as heat capacity and thermal expansion. Unfortunately, the experimental determination of Grüneisen parameter (γ), defined in either way, is extremely difficult; the macroscopic definition requires a detailed knowledge of the phonon dispersion spectrum of the material, whereas the microscopic definition requires experimental measurements of thermodynamic properties at high pressure and temperature. As a result of the difficulty associated with obtaining experimentally an accurate value for Grüneisen parameter (γ), (a number of more approximate expressions have been suggested by Poirier [12]) many of these relate Grüneisen parameter (γ) at atmospheric pressure ($P=0$) to the first derivative of the bulk modulus with respect to pressure K_T' via $\gamma=(1/2)K_T'-X$, where X is constant. These relations may be expanded to take into account the variation of Grüneisen parameter (γ) with pressure. In these more general cases, Grüneisen parameter $\gamma(P)$ is a function of the equation of state. Despite the intrinsic relationship between Grüneisen parameter (γ) and equation of state [13], it is frequently the case that the choice of the functional form of both the Grüneisen parameter and the equation of state to which it should be related are made independent of each other, and somewhat arbitrary; this has resulted in literature in which there are wide range of values of Grüneisen parameter (γ) for many geologically relevant materials. It is therefore, important to investigate more carefully how the value of Grüneisen parameter (γ) and its compressional behaviour are affected by:

(1) The choice of the formulation of Grüneisen parameter (γ).
(2) The use of different equation of state's (EOS's).

We shall firstly review the various formulations of Grüneisen parameter (γ), starting how they may be obtained directly from the equation of state. In the present work the Grüneisen parameter has been estimated at different compression for six different BMGs, viz. $Zr_{41}Ti_{14}Cu_{12.5}Ni_{10}Be_{22.5}$, $Zr_{41}Ti_{14}Cu_{12.5}Ni_{9}Be_{22.5}C_1$, $Zr_{48}Nb_8Cu_{12}Fe_8Be_{24}$, $(Zr_{0.59}Ti_{0.06}Cu_{0.22}Ni_{0.13})_{85.7}Al_{14.3}$, $SiO_2{\cdot}TiO_2$ and $Pd_{39}Ni_{10}Cu_{30}P_{21}$ using four phenomenological isothermal equations of state Birch–Murnaghan III EOS, Vinet and Rydburg EOS, Brennan–Stacey EOS and Hama–Suito EOS. A comparative study has also been made among the calculated values of Grüneisen Parameter to test the validity of various equations of states.

2. The Grüneisen parameter

The free volume expression for Grüneisen parameter (γ) was derived by Vaschenk and Zubarev [14] and Irvine and Stacey [13] followed by the path suggested by Brillouin [15], who showed that the thermal pressure may be considered as that required to keep the volume constant as the temperature raised, they expended the "mutual forces between the atoms at separation r" in a series expansion around r_0 to quadratic terms and found the pressure necessary to keep ΔV zero at given T, and solved for Grüneisen parameter (γ)

$$\gamma_{VZ}=\frac{(1/2)K'-(5/6)+(2/9)(P/K_T)}{1-(4/3)(P/K_T)} \quad (1)$$

where the subscript refers to Vashchenko's and Zubarev's approach.

Further, Stacey assumed that the correlation of motions along a bond was the same with respect to dilation as that of those transverse to the bond. Thus, Barton and Stacey [16], fond correlation for Grüneisen parameter (γ) leading to

$$\gamma_{ba\text{-}s}=\frac{(1/2)K'-\frac{1}{6}-(f/3)[1-((1/3)(P/K_T))]}{1-(4/3)(P/K_T)} \quad (2)$$

where $f=2.35$ not 2 as in Eq. (1)
At $P=0$, Eq. (2) reduces to $\gamma_{ba\text{-}s}=(K'/2)-0.95$.

3. Computation of Grüneisen parameter (γ) from equation of state

The four phenomenological forms of isothermal equation of state as derived from lattice potential theory [17–19] are as follows:

$$P=\frac{3}{2}K_0[x^{-7}-x^{-5}]\left[1+\frac{3}{4}(K_0'-4)(x^{-2}-1)\right] \quad (3)$$

$$P=\frac{3K_0x^{-4}}{3K_0'-5}\left[\exp\left\{\frac{(3K_0'-5)(1-x^3)}{3}\right\}-1\right] \quad (4)$$

$$P=3K_0x^{-2}[1+(1-x)(1+\eta x)]\exp[\eta(1-x)] \quad (5)$$

$$P=3K_0x^{-5}(1-x)\exp\left[\frac{3}{2}(K_0'-3)(1-x)+\left(z-\frac{3}{2}\right)(1-x)^2\right] \quad (6)$$

where $x=(V/V_0)^{1/3}$ and $\eta=(3/2)(K_0'-1))$ and $z=(3/8)(K_0'-1)(K_0'+3)-(3/5)K_0'^2+(1/3)$

V is the volume at pressure P and V_0 is the volume at zero pressure, K_0 and K_0' are the isothermal bulk modulus and its first pressure derivative at zero pressure respectively. Eq. (3) is the Birch–Murnaghan (III) EOS derived, using the finite strain theory [20], Eq. (4) is the Brennan–Stacey EOS derived using the thermodynamic formulation for the Grüneisen parameter [21,22]. Eq. (5) is the Vinet–Rydburg EOS based on universal relationship between binding energy and interatomic separation for solids [23,24].

Expressions for isothermal bulk modulus corresponding to Eqs. (3)–(6) obtained using the relationship $K_T=-V(\partial P/\partial V)_T$ are given as follows:

$$K_T=\frac{K_0}{2}[7x^{-7}-5x^{-5}]+\frac{3}{8}K_0(K_0'-4)(9x^{-9}-14x^{-7}+5x^{-5}) \quad (7)$$

$$K_T=K_0x^{-1}\exp\left\{\left(K_0'-\frac{5}{3}\right)(1-x^{1/3})\right\}+\frac{4}{3}P \quad (8)$$

$$K_T=K_0x^{-2}[1+(\eta x+1)(1-x)]\exp\{\eta(1-x)\} \quad (9)$$

$$K_T=\frac{P}{3}\left[\left\{5+\frac{x}{1-x}\right\}+x\left\{\frac{3}{2}(K_0'-1)+2z(1-x)+3x-6\right\}\right] \quad (10)$$

The corresponding expression for $K_T'=(\partial K_T/\partial P)$ obtained from Eqs. (6)–(8) are written as follows:

$$K_T'=\frac{K_0}{8K_T}\left[(K_0'-4)(81x^{-9}-98x^{-7}+25x^{-5})+\frac{4}{9}(49x^{-7}-25x^{-5})\right] \quad (11)$$

Table 2
Calculated values of pressure (P), isothermal bulk modulus (K_T), its first pressure derivative (K_T'), Barton–Stacey Grüneisen parameter ($\gamma_{ba\text{-}s}$) and Anderson–Grüneisen parameter (δ_T) at different compressions (V/V_0) for $Zr_{41}Ti_{14}Cu_{12.5}Ni_{10}Be_{22.5}$ using (a) Birch–Murnaghan III EOS, (b) Brennan–Stacey EOS, (c) Vinet–Rydburg EOS, (d) Hama–Suito EOS at $T = T_0 = 300$ K.

V/V_0	P (a) (GPa)	K (a) (GPa)	K'	$\gamma_{ba\text{-}s}$ (a)	P (b) (GPa)	K (b) (GPa)	K' (b)	$\gamma_{ba\text{-}s}$ (b)	P (c) (GPa)	K (c) (GPa)	K' (c)	$\gamma_{ba\text{-}s}$ (c)	P (d) (GPa)	K (d) (GPa)	K' (d)	$\gamma_{ba\text{-}s}$ (d)
1.00	0.00	114.10	4.06	1.08	0.00	114.10	4.06	1.08	0.00	114.10	4.06	1.08	0.00	114.10	4.06	1.08
0.90	14.89	171.68	3.72	1.05	14.84	164.73	3.52	0.95	14.85	170.29	3.57	0.97	14.82	169.54	3.50	0.93
0.80	40.11	261.66	3.46	1.03	39.41	236.70	3.08	0.82	39.57	253.37	3.20	0.87	39.29	249.25	3.07	0.79
0.70	84.26	409.02	3.25	1.00	80.56	341.36	2.71	0.68	81.42	379.85	2.89	0.77	80.07	366.82	2.73	0.67
0.60	165.66	665.60	3.08	0.98	151.18	498.77	2.39	0.54	154.56	580.05	2.62	0.67	149.80	546.64	2.46	0.55
0.50	327.61	1151.45	2.94	0.96	277.39	747.42	2.11	0.40	288.96	914.10	2.38	0.56	274.44	836.26	2.22	0.44
0.40	688.78	2189.18	2.83	0.94	518.25	1170.66	1.86	0.24	555.43	1514.74	2.16	0.44	513.74	1339.97	2.02	0.32
0.30	1654.55	4861.28	2.73	0.92	1030.39	1983.21	1.66	0.05	1151.35	2724.03	1.93	0.29	1030.71	2329.91	1.84	0.21
0.20	5231.16	14,440.94	2.65	0.91	2357.88	3917.97	1.49	−0.23	2794.46	5675.31	1.70	0.08	2415.72	4753.42	1.69	0.09
0.10	33,669.72	88,754.91	2.60	0.91	7825.80	11,417.86	1.38	−0.93	9960.05	16,589.17	1.42	−0.43	8542.47	14,619.28	1.57	−0.05

Table 3
Calculated values of pressure (P), isothermal bulk modulus (K_T), its first pressure derivative (K_T'), Barton–Stacey Grüneisen parameter ($\gamma_{ba\text{-}s}$) and Anderson–Grüneisen parameter (δ_T) at different compressions (V/V_0) for $Zr_{41}Ti_{14}Cu_{12.5}Ni_9Be_{22.5}C_1$ using (a) Birch–Murnaghan (III) EOS, (b) Brennan–Stacey EOS, (c) Vinet–Rydburg EOS, (d) Hama–Suito EOS at $T = T_0 = 300$ K.

V/V_0	P (a) (GPa)	K (a) (GPa)	K'	$\gamma_{ba\text{-}s}$ (a)	P (b) (GPa)	K (b) (GPa)	K' (b)	$\gamma_{ba\text{-}s}$ (b)	P (c) (GPa)	K (c) (GPa)	K' (c)	$\gamma_{ba\text{-}s}$ (c)	P (d) (GPa)	K (d) (GPa)	K' (d)	$\gamma_{ba\text{-}s}$ (d)
1.00	0.00	107.30	3.94	1.02	0.00	107.30	3.94	1.02	0.00	107.30	3.94	1.02	0.00	107.30	3.94	1.02
0.90	13.91	159.50	3.61	0.99	13.86	153.17	3.43	0.89	13.88	158.35	3.48	0.92	13.85	157.71	3.41	0.88
0.80	37.18	239.95	3.35	0.96	36.59	217.85	3.00	0.77	36.73	233.17	3.11	0.82	36.49	229.71	3.00	0.75
0.70	77.34	369.57	3.14	0.93	74.26	311.23	2.65	0.64	75.04	346.08	2.82	0.72	73.91	335.28	2.68	0.63
0.60	150.20	590.81	2.96	0.90	138.29	450.77	2.34	0.50	141.31	523.17	2.56	0.62	137.38	495.89	2.41	0.52
0.50	292.22	999.20	2.81	0.87	251.71	670.00	2.07	0.36	261.83	815.82	2.33	0.52	250.02	753.37	2.19	0.41
0.40	600.44	1841.94	2.68	0.84	466.32	1041.50	1.83	0.21	498.16	1336.53	2.11	0.40	464.81	1199.36	1.99	0.31
0.30	1392.55	3904.48	2.55	0.80	919.00	1752.21	1.64	0.02	1020.19	2372.73	1.89	0.25	925.96	2073.13	1.82	0.19
0.20	4135.43	10,685.09	2.42	0.75	2083.78	3439.73	1.48	−0.26	2438.68	4867.19	1.66	0.04	2154.45	4207.67	1.68	0.08
0.10	22,746.87	53,452.07	2.22	0.63	6850.61	9964.32	1.38	−0.97	8505.25	13,929.24	1.39	−0.52	7563.47	12,891.23	1.57	−0.06

Table 4
Calculated values of pressure (P), isothermal bulk modulus (K_T), its first pressure derivative (K_T'), Barton–Stacey Grüneisen parameter ($\gamma_{ba\text{-}s}$) and Anderson–Grüneisen parameter (δ_T) at different compressions (V/V_0) for $Zr_{40}Nb_3Cu_{12}Fe_8Be_{24}$ using (a) Birch–Murnaghan (III) EOS, (b) Brennan–Stacey EOS, (c) Vinet–Rydburg EOS, (d) Hama–Suito EOS at $T = T_0 = 300$ K.

V/V_0	P (a) (GPa)	K (a) (GPa)	K'	$\gamma_{ba\text{-}s}$ (a)	P (b) (GPa)	K (b) (GPa)	K' (b)	$\gamma_{ba\text{-}s}$ (b)	P (c) (GPa)	K (c) (GPa)	K' (c)	$\gamma_{ba\text{-}s}$ (c)	P (d) (GPa)	K (d) (GPa)	K' (d)	$\gamma_{ba\text{-}s}$ (d)
1.00	0.00	113.60	4.10	1.10	0.00	113.60	4.10	1.10	0.00	113.60	4.10	1.10	0.00	113.60	4.10	1.10
0.90	13.91	171.61	3.75	1.07	14.80	164.63	3.55	0.97	14.81	170.19	3.61	0.99	14.79	169.41	3.53	0.95
0.80	37.18	262.68	3.49	1.05	39.41	237.36	3.11	0.83	39.56	254.08	3.22	0.89	39.27	249.82	3.10	0.81
0.70	77.34	412.54	3.28	1.03	80.75	343.40	2.73	0.70	81.61	382.19	2.91	0.78	80.21	368.67	2.75	0.68
0.60	150.20	675.07	3.12	1.00	151.92	503.23	2.40	0.55	155.34	585.58	2.64	0.68	150.39	550.76	2.47	0.56
0.50	292.22	1175.91	2.98	0.98	279.50	756.17	2.12	0.41	291.27	926.06	2.40	0.57	276.13	844.49	2.23	0.45
0.40	600.44	2256.08	2.87	0.97	523.67	1187.39	1.87	0.25	561.80	1540.38	2.17	0.45	518.07	1355.98	2.03	0.33
0.30	1392.55	5075.39	2.78	0.95	1044.26	2016.27	1.66	0.05	1169.27	2782.07	1.95	0.30	1041.80	2362.24	1.85	0.21
0.20	4135.43	15,399.39	2.71	0.95	2397.02	3991.83	1.50	−0.22	2852.40	5826.34	1.71	0.09	2447.41	4827.19	1.69	0.09
0.10	22,746.87	98,957.82	2.67	0.96	7981.21	11,656.65	1.38	−0.91	10,240.40	17,151.18	1.42	−0.40	8674.06	14,862.51	1.57	−0.05

Table 5
Calculated values of pressure (P), isothermal bulk modulus (K_T), its first pressure derivative (K_T'), Barton–Stacey Grüneisen parameter ($\gamma_{ba\text{-}s}$) and Anderson–Grüneisen parameter (δ_T) at different compressions (V/V_0) for $(Zr_{0.59}Ti_{0.06}Cu_{0.22}Ni_{0.13})_{0.57}Al_{14.3}$ using (a) Birch–Murnaghan (III) EOS, (b) Brennan–Stacey EOS, (c) Vinet–Rydburg EOS, (d) Hama–Suito EOS at $T = T_0 = 300$ K.

V/V_0	P (a) (GPa)	K (a) (GPa)	K'	$\gamma_{ba\text{-}s}$ (a)	P (b) (GPa)	K (b) (GPa)	K' (b)	$\gamma_{ba\text{-}s}$ (b)	P (c) (GPa)	K (c) (GPa)	K' (c)	$\gamma_{ba\text{-}s}$ (c)	P (d) (GPa)	K (d) (GPa)	K' (d)	$\gamma_{ba\text{-}s}$ (d)
1.00	0.00	112.60	4.34	1.22	0.00	112.60	4.34	1.22	0.00	112.60	4.34	1.22	0.00	112.60	4.34	1.22
0.90	14.92	174.19	3.97	1.19	14.86	166.92	3.75	1.07	14.87	172.52	3.80	1.10	14.84	171.59	3.70	1.04
0.80	40.90	273.20	3.69	1.17	40.09	245.65	3.27	0.93	40.24	262.91	3.38	0.98	39.89	257.69	3.23	0.89
0.70	87.78	440.54	3.48	1.15	83.35	362.24	2.86	0.78	84.22	403.40	3.05	0.87	82.49	386.43	2.86	0.75
0.60	177.16	742.84	3.31	1.13	159.26	540.40	2.51	0.63	162.90	630.57	2.76	0.76	156.65	585.72	2.55	0.62
0.50	362.16	1341.06	3.18	1.11	297.85	825.73	2.20	0.47	310.97	1018.29	2.51	0.65	291.36	910.05	2.29	0.49
0.40	795.53	2691.18	3.07	1.10	567.78	1316.98	1.93	0.30	612.19	1732.69	2.27	0.52	553.86	1478.89	2.07	0.37
0.30	2032.87	6430.77	2.99	1.09	1152.87	2268.71	1.70	0.10	1305.44	3210.94	2.03	0.38	1128.60	2603.80	1.88	0.24
0.20	7082.02	21,340.27	2.93	1.08	2696.61	4551.24	1.52	−0.18	3283.10	6936.49	1.78	0.17	2686.18	5366.74	1.71	0.10
0.10	55,059.28	161,078.35	2.91	1.09	9155.64	13,456.20	1.39	−0.84	12,309.88	21,302.90	1.48	−0.26	9633.24	16,602.12	1.57	−0.05

Table 6
Calculated values of pressure (P), isothermal bulk modulus (K_T), its first pressure derivative (K_T'), Barton–Stacey Grüneisen parameter ($\gamma_{ba\text{-}s}$) and Anderson–Grüneisen parameter (δ_T) at different compressions (V/V_0) for $SiO_2{\cdot}TiO_2$ using (a) Birch–Murnaghan (III) EOS, (b) Brennan–Stacey EOS, (c) Vinet–Rydburg EOS, (d) Hama–Suito EOS at $T = T_0 = 300$ K.

V/V_0	P (a) (GPa)	K (a) (GPa)	K'	$\gamma_{ba\text{-}s}$ (a)	P (b) (GPa)	K (b) (GPa)	K' (b)	$\gamma_{ba\text{-}s}$ (b)	P (c) (GPa)	K (c) (GPa)	K' (c)	$\gamma_{ba\text{-}s}$ (c)	P (d) (GPa)	K (d) (GPa)	K' (d)	$\gamma_{ba\text{-}s}$ (d)
1.00	0.00	34.20	−7.71	−4.81	0.00	34.20	−7.71	−4.81	0.00	34.20	−7.71	−4.81	0.00	34.20	−7.71	−4.81
0.90	1.61	−9.49	62.57	24.71	2.55	16.80	−5.13	−4.36	2.42	14.00	−9.53	−7.37	2.36	12.63	−11.98	−9.18
0.80	−4.88	−112.74	10.77	4.72	4.16	10.79	−2.15	−3.96	3.35	3.15	−18.97	24.33	3.02	0.18	−365.15	8.56
0.70	−33.87	−348.49	6.97	2.94	5.52	9.41	−0.03	−3.71	3.37	−1.89	11.16	1.23	2.63	−4.92	3.23	0.31
0.60	−124.99	−898.38	5.52	2.27	7.04	10.19	0.92	−3.95	2.92	−3.54	0.94	−0.33	1.80	−5.29	−1.22	−1.13
0.50	−397.87	−2269.09	4.73	1.91	9.11	12.46	1.22	−5.84	2.27	−3.42	−0.90	−0.83	0.98	−3.57	−2.85	−1.79
0.40	−1272.07	−6120.65	4.21	1.68	12.33	16.56	1.31	−13.67	1.60	−2.57	−1.54	−1.03	0.41	−1.69	−3.75	−2.18
0.30	−4612.04	−19,397.41	3.84	1.51	18.14	24.23	1.33	−45.38	1.01	−1.59	−1.76	−1.08	0.12	−0.53	−4.28	−2.42
0.20	−22,940.89	−86,182.62	3.55	1.38	31.17	41.58	1.33	−193.54	0.55	−0.77	−1.75	−1.03	0.02	−0.09	−4.51	−2.51
0.10	−268,650.68	−911,684.13	3.29	1.27	78.56	104.76	1.33	−1239.81	0.23	−0.25	−1.53	−0.87	0.00	0.00	−4.28	−2.38

Table 7
Calculated values of pressure (P), isothermal bulk modulus (K_T), its first pressure derivative (K_T'), Barton–Stacey Grüneisen parameter ($\gamma_{ba\text{-}s}$) and Anderson–Grüneisen parameter (δ_T) at different compressions (V/V_0) for $Pd_{39}Ni_{10}Cu_{30}P_{21}$ using (a) Birch–Murnaghan III EOS, (b) Brennan–Stacey EOS, (c) Vinet–Rydburg EOS, (d) Hama–Suito EOS at $T = T_0 = 300$ K.

V/V_0	P (a) (GPa)	K (a) (GPa)	K'	$\gamma_{ba\text{-}s}$ (a)	P (b) (GPa)	K (b) (GPa)	K' (b)	$\gamma_{ba\text{-}s}$ (b)	P (c) (GPa)	K (c) (GPa)	K' (c)	$\gamma_{ba\text{-}s}$ (c)	P (d) (GPa)	K (d) (GPa)	K' (d)	$\gamma_{ba\text{-}s}$ (d)
1.00	0.00	159.10	6.28	2.19	0.00	159.10	6.28	2.19	0.00	159.10	6.28	2.19	0.00	159.10	6.28	2.19
0.90	23.27	292.86	5.39	1.98	23.26	283.38	5.33	1.95	23.22	291.26	5.29	1.92	23.09	287.05	5.04	1.78
0.80	70.75	532.61	4.81	1.81	70.40	494.16	4.59	1.71	70.04	520.72	4.62	1.70	68.31	493.16	4.21	1.46
0.70	169.37	983.68	4.41	1.68	165.95	856.21	3.98	1.47	164.90	931.85	4.12	1.52	155.18	827.87	3.59	1.19
0.60	384.23	1891.43	4.10	1.58	363.24	1491.46	3.43	1.23	363.01	1702.17	3.72	1.35	322.89	1381.10	3.08	0.95
0.50	892.09	3899.41	3.85	1.49	785.67	2645.07	2.93	0.98	800.88	3239.13	3.36	1.18	655.39	2324.07	2.65	0.72
0.40	2257.76	8998.87	3.65	1.42	1746.66	4862.82	2.47	0.73	1860.56	6595.69	3.03	1.02	1350.43	4015.69	2.27	0.50
0.30	6789.06	25,077.24	3.48	1.35	4166.47	9574.60	2.05	0.45	4826.80	15,006.54	2.70	0.85	2947.79	7331.83	1.94	0.26
0.20	28,799.50	99,554.96	3.33	1.29	11,520.62	21,736.22	1.70	0.13	15,528.87	41,618.11	2.35	0.64	7342.88	15,055.18	1.64	−0.01
0.10	291,530.56	947,055.80	3.19	1.23	46,482.80	72,089.63	1.44	−0.42	82,714.15	180,382.01	1.91	0.32	25,970.67	42,754.81	1.41	−0.45

$$K'_T = \left(1 - \frac{4}{3}\frac{P}{K_T}\right)\left\{\left(K'_0 - \frac{5}{3}\right)x^3 + \frac{5}{3}\right\} + \frac{16}{9}\frac{P}{K_T} \quad (12)$$

$$K'_T = \frac{1}{3}\left[\frac{x(1-\eta) + 2\eta x^2}{1 + (\eta x + 1)(1-x)} + \eta x + 2\right] \quad (13)$$

$$K'_T = \frac{K_T}{P} - \frac{1}{3} + \frac{P}{9K_T}\left[x^2\left\{(2z-3) - \frac{1}{(1-x)^2}\right\} + 5\right] \quad (14)$$

Thus Eqs. (3), (7) and (11) represent the Birch–Murnaghan (III) EOS, Eqs. (4), (8) and (12) represent the Brennan–Stacey EOS, Eqs. (5), (9) and (13) represent the Vinet–Rydburg EOS and Eqs. (6), (10) and (14), represent the Hama–Suito EOS respectively.

4. Results and discussion

In the present work we have described four different forms of EOS; Eqs. (3), (7) and (11) represent the Birch–Murnaghan (III) EOS's, Eqs. (4), (8) and (12) represent the Brennan–Stacey EOS's, Eqs. (5), (9) and (13) represent the Vinet–Rydburg EOS's and Eqs. (6), (10) and (14), represent the Hama–Suito EOS's respectively. All the four EOS contain only two parameters K_0 and K'_0 both at zero pressure. It has been the usual practice to adjust or to fit the parameters K_0 and K'_0 in order to achieve the agreement with the experimental values. This procedure of fitting does not provides a useful insight for the physical EOS. In order to make a real test of EOS we have used experimental values of K_0 and K'_0 for given bulk metallic glasses. These values of K_0 and K'_0 have been recommended by Anderson [20]. The values of pressure P for six different BMG's, viz. $Zr_{41}Ti_{14}Cu_{12.5}Ni_{10}Be_{22.5}$, $Zr_{41}Ti_{14}Cu_{12.5}Ni_9Be_{22.5}C_1$, $Zr_{48}Nb_8Cu_{12}Fe_8Be_{24}$, $(Zr_{0.59}Ti_{0.06}Cu_{0.22}Ni_{0.13})_{85.7}Al_{14.3}$, $SiO_2{\cdot}TiO_2$ and $Pd_{39}Ni_{10}Cu_{30}P_{21}$, were computed for given increments of V/V_0 by using Eqs. (3)–(6). The value of input parameter, K_0 and K'_0 are taken from literature [25] are shown in Table 1. Using the values of pressure P computed from Eqs. (3)–(6) for six different BMG's, the values of first pressure derivative of bulk modulus (K_T) at constant temperature are computed from Eqs. (7)–(10). Substituting these values P and K_T, in Eqs. (11)–(14), the value of K'_T is obtained which is shown in Tables 2–7. Substituting the values of P, K_T and K'_T, in Eq. (2) the value of $\gamma_{ba\text{-}s}$ were calculated which is shown in Tables 2–7. A graph is plotted between the Grüneisen parameter (γ) versus V/V_0 which are shown in Figs. 1–6 leading to the following generalisation.

The graphs plotted between Grüneisen parameter (γ) versus V/V_0 which are obtained by Birch–Murnaghan (III) EOS and Hama–Suito EOS are straight line for most of the BMG's except $SiO_2{\cdot}TiO_2$ but it is curved for the values obtained by Vinet–Rydburg EOS and Brennan–Stacey EOS. It has been noted that to a good approximation the ratio γ/Ω (where $\Omega = V/V_0$) of Grüneisen parameter to volume is constant for solids [26]. Fang and Rong [27] have calculated the melting temperature under high pressure with the assumption that γ/Ω is constant, has been frequently used in work on shock compression of metals.

The expression γ/Ω leads to equation of straight line. Hence the graph between Grüneisen parameter (γ) versus Ω must be a straight line which strongly supports the Birch–Murnaghan (III) EOS and Hama–Suito EOS both under low and high compressions whereas Vinet–Rydburg EOS and Brennan–Stacey EOS are applicable only at high compression ratio. Thus, Birch–Murnaghan (III) EOS and Hama–Suito EOS are compatible both low and high compression ranges for calculating Grüneisen parameter whereas Vinet–Rydburg EOS and Brennan–Stacey EOS are incompatible for calculating the Grüneisen parameter using Eq. (2) at low compression ranges.

In spite of this reservation on Grüneisen parameter (γ) the evidence supports the idea that the exponential variation of Grüneisen parameter (γ) with volume is much different at high pressure in comparison to low pressure. This conclusion is also supported by the work of Kopyshev [28], who investigated the behaviour of Grüneisen parameter (γ) using Fermi-Dirac theory. He found that Grüneisen parameter (γ) approached the limiting value of 1/2 at a condition of vanishing volume. This conclusion also agrees with the results of Rice [29], by assuming that both the adiabatic bulk modulus and Grüneisen parameter (γ) are independent of temperature. He found that

$$\frac{\gamma}{V} = \frac{\gamma_0}{V_0}\left[1 + \gamma_0\left(1 - \frac{V}{V_0}\right)\right]^{-2}$$

Using a harmonic theory, Pastine [30] computed the curve for Grüneisen parameter (γ) versus V, which shows smaller exponent at higher pressure.

It is not always necessary to make a prior assumption of the volume dependence of Grüneisen parameter (γ) in order to compute temperature effect in shock waves. Another way tried by Takeuchi and Kanamori [31] makes an assumption about thermal equation of state, and the empirical relationship γ versus V/V_0 For example, Takeuchi and Kanamori [31] assumed that the γ versus V/V_0 curve is linear and that the pressure–energy relationship is given by one of the Mie–Grüneisen equation. It is interesting to note that the values of Grüneisen parameter (γ) computed by their method indicates that the exponential power of V for Grüneisen parameter (γ) is higher at low pressure than at high pressure. Such evidences strongly support the Grüneisen parameter as calculated by using Hama–Suito EOS. Thus Hama–Suito EOS is the best EOS for calculating Grüneisen parameter both at high and low compression ranges for BMG's.

References

[1] W. Clement, R.H. Willens, P. Duwez, Nature 187 (1960) 869.
[2] M.X. Pan, W.H. Wang, D.Q. Zhao, Z.X. Bao, W.X. Zhang, S.Z. Zhang, J. Phys. Condens. Matter 14 (2002) 5665.
[3] W.L. Johnson, Prog. Mater. Sci. 30 (1986) 81.
[4] W.H. Wang, C. Dong, C.H. Shek, Mater. Sci. Eng. 44 (2005) 45.
[5] S. Kavesh, in: J.J. Gillman, H.L. Leamy (Eds.), Metallic Glasses, ASM International, Metals Park, OH, 1978 (Chapter 2).
[6] J. Xu, M.H. Manghnani, Phys. Rev. B 45 (1992) 640.
[7] R.C. Purdom, E.W. Prohofsky, Phys. Rev. B 2 (1970) 551.
[8] M. Grimsditch, K.E. Gray, R. Bhadra, L.E. Rehn, Phys. Rev. B 35 (1987) 883.
[9] Z.Y. Shen, G.Y. Chen, Y. Zhang, X.J. Yin, Phys. Rev. B 39 (1989) 2714.
[10] W.K. Wang, H. Iwasaki, K. Fukamichi, Mater. J. Sci. 15 (1980) 2701.
[11] W.H. Wang, D.W. He, D.Q. Zhao, Y.S. Yao, Appl. Phys. Lett. 75 (1999) 2770.
[12] J.P. Poirier, Introduction to Physics of Earth's Interior, Cambridge Univ. Press, Cambridge, 1991.
[13] R.D. Irvine, F.D. Stacey, Phys. Earth Planet Interior 11 (1975) 157.
[14] V.Y. Vaschenk, V.N. Zubarev, Sov. Phys. Solid State (Engl. Transl.) 5 (1963) 653.
[15] L. Brillouin, Wave Propagation in Periodic Structures, McGraw Hill Book Co. Inc., New York, 1946, p. 246.
[16] M.A. Barton, F.D. Stacey, Phys. Earth Planet Interior 39 (1985) 167.
[17] M.S. Kumar, B.S. Sharma, Ind. J. Pure Appl. Phys. 48 (2010) 282.
[18] B.J. Brennan, F.D. Stacey, J. Geophys. Res. 84 (1979) 5535.
[19] A.K. Upadhyay, B.S. Sharma, Ind. J. Pure Appl. Phys. 47 (2009) 362.
[20] O.L. Anderson, Equation of State of Solids for Geophysics and Ceramic Science, Oxford University Press, New York, 1995.
[21] F.D. Stacey, B.J. Brennan, R.D. Irvine, Geophys. Surv. 4 (1981) 189.
[22] H.K. Rai, S.P. Shukla, A.K. Misra, A.K. Pandey, Electron. J. Chem. 5 (2008) 385–394.
[23] P. Vinet, J. Ferrante, J.R. Smith, J.H. Rose, J. Phys. C 92 (1986) L467.
[24] P. Vinet, J. Ferranate, J.H. Rose, J.R. Smith, J. Phys. Res. 19 (1987) 9319.
[25] W.H. Wang, P. Wen, L.M. Wang, Y. Zhang, M.X. Pan, D.Q. Zhao, R.J. Wang, Appl. Phys. Lett. 79 (24) (2001) 3947.
[26] R. Boehler, Phys. Rev. B 11 (1983) 6754.
[27] Z.H. Fang, L. Rong, J. Phys. Condens. Matter 6 (1994) 6937.
[28] V.P. Kopyshev, Dokl. Soviet Phys., Eng. Trans. 10 (4) (1965) 338.
[29] M.H. Rice, J. Phys. Chem. Solids 26 (1965) 483.
[30] D.J. Pastine, Phys. Rev. 138A (1965) 767.
[31] H. Takeuchi, H. Kanamori, J. Geophys. Res. 71 (1966) 3985.